CHEMIJA. 2022. Vol. 33. No. 2. P. 27–34

A novel method for the formation of bioceramic nano-calcium hydroxyapatite coatings using sol-gel and dissolution-precipitation processing

Rasa Karalkevičienė[1],

Greta Briedytė[1],

Tomas Murauskas[1],

Mantas Norkus[1],

Aleksej Žarkov[1],

Jen-Chang Yang[2],

Aivaras Kareiva[1*]

[1] *Institute of Chemistry, Vilnius University, 24 Naugarduko Street, 03225 Vilnius, Lithuania*

[2] *Graduate Institute of Nanomedicine and Medical Engineering, College of Biomedical Engineering, Taipei Medical University, Taipei 11052, Taiwan*

The wet chemistry route has been developed to prepare calcium hydroxyapatite ($Ca_{10}(PO_4)_6(OH)_2$, (HA)) thin films on a silicon substrate using the novel low-temperature sol-gel and dissolution-precipitation approach. The calcium carbonate thin films on the silicon substrate were obtained by spin-coating technique when substrates were repeatedly coated with 10, 20 and 30 layers of sol-gel solution. The composites formed of crystalline and amorphous $CaCO_3$ were obtained by calcination of the coatings for different time at 600°C. A dissolution-precipitation procedure was used for the preparation of calcium hydroxyapatite thin films on silicon substrate at 80°C. The obtained synthesis products were characterised by X-ray powder diffraction (XRD) analysis, scanning electron microscopy (SEM) and Raman spectroscopy.

Keywords: calcium hydroxyapatite, thin films, silicon substrate, spin-coating, sol-gel processing

INTRODUCTION

There is a need to reconstruct damaged hard tissue for several reasons that include traumatic or non-traumatic events, congenital abnormalities, or disease. Damaged tissues stemming from these events can become a major issue in orthopedic, dental and maxillofacial surgery. A study on numerous biomaterials revealed that calcium phosphates had been used in hard tissue reconstruction for more than six decades. Calcium hydroxyapatite ($Ca_{10}(PO_4)_6(OH)_2$, HA) was the primary material used in orthopedics and dentistry [1, 2].

HA crystals are present in the human body both inside bone and teeth. In terms of the human bone, the HA crystals as a bioactive ceramic cover 65 to 70% by weight of the bone. Furthermore, the architecture of the bone comprises type-I collagen as an organic component and the HA as an inorganic component. These two components form a composite structure at the nanoscale, in which nano-HA is interspersed in the collagen network. This composite forms mineralised collagen and is the precursor of biological mineralised tissue from tendons and skin to hard mineralised tissues such as bone and teeth. Moreover, in the bone, the HA crystals present in the shape of plates or needles are about 40 to 60 nm long, 20 nm wide, and 1.5 to

* Corresponding author. Email: aivaras.kareiva@chf.vu.lt

5 nm thick [3, 4]. The arrangement of different HA crystalline sizes and shapes provides support for this tissue's structural stability, hardness and function [5, 6].

HA application in orthopedics can vary from bone defects repair and bone augmentation to coatings for human body metallic implants. The HA-based implants can provide an interlocked porous structure [7–9]. This structure can act as the extracellular matrix, promoting the natural process of cellular development and tissue regeneration [9, 10]. Furthermore, HA can enhance the osseointegration process by promoting a rigid anchorage between the implant and the surrounding tissue without the growth of fibrous tissue. The successful osseointegration retains the bone anchorage for a long period, hence completely restoring functional ability [11, 12].

HA coatings on different substrates are being widely used in orthopaedics and dentistry [13–19]. Many preparation techniques are used currently in coating of HA onto different substrates [18, 20]. Hydroxyapatite synthesised by different methods has different surface morphology and the products also have different chemical properties [25–29]. In order to produce a coating that is more resistant to physiological conditions, various new methods are being sought for the modern synthesis of HA layers that replicate bone tissue. Si could be used for the formation of an interfacial layer on the metal alloys to increase the adhesion strength of biomaterials substantially [26]. Cha et al. [27] also showed that silicon could be used for improving the biological performance of ZrO_2 substrate. The results revealed that Zr-Si-HA substrates are very promising biomaterials for bone tissue engineering. Interestingly, Hiebl et al. [28] reported that the Si-based substrate is also a promising candidate for the formation of materials which are aimed to be used in cardiovascular tissue engineering approaches. Moreover, silicon substrates modified with graphene oxides could be applied to control living cells on these substrates [29]. These substrates are important for the development of bio-applications, including biosensors and implant biomaterials. Recently, samarium-doped hydroxyapatite (Sm-HA) coatings were fabricated on the Si substrate [30]. This study showed that the Sm-HA samples on the Si substrate are good candidates for the development of new antimicrobial agents. A natural rubber-calcium phosphate hybrid for applications as bioactive coatings was also synthesised on the Si substrate [31]. Finally, silicon or silicon-containing composites are very useful substrates for the application for blood-contacting implants, for the patterned cell culture *in vitro* or to improve cell response [32–34].

In this paper, we report the novel low-temperature sol-gel synthetic and dissolution-precipitation approach and the characterisation of HA thin films on a silicon substrate using a spin-coating technique.

EXPERIMENTAL

Firstly, calcium carbonate ($CaCO_3$) layers on silicon substrates were fabricated by sol-gel synthesis. Silicon substrates were washed with Piranha solution (3 parts of concentrated sulfuric acid and 1 part of 30% hydrogen peroxide solution) and distilled water. In the sol-gel process, 20 ml of 2-propanol (99.0%; Alfa Aesar) were mixed with 1.8 ml of acetylacetone, $C_5H_8O_2$ (99.9%; Merck) with stirring at room temperature. An appropriate amount (1.0920 g) of calcium nitrate tetrahydrate ($Ca(NO_3)_2{\cdot}4H_2O$) (99.0%; Fluka) was added to the solution and stirred for 1 h until the material dissolved [35]. The solution used for coating the silicon substrates was mixed with the polyvinyl alcohol (PVA) (PVA7200, 99.5%; Aldrich) solution in a ratio of 5:3. A polyvinyl alcohol (PVA) solution was obtained by dissolving 0.5 g of polyvinyl alcohol (PVA) in 49.5 ml of distilled water with stirring at 90°C for 1 h. The silicon substrate was repeatedly coated with 10, 20 and 30 layers of solution by the spin-coating method using two different spinning procedures (A) and (B) (Table). After the evaporation of solvent the substrates were dried in an oven for 10 min at 200°C and heated at 600°C for 5 h with a heating rate of 5°C/min. Calcium hydroxyapatite coatings were synthesised by the low-temperature dissolution-precipitation method. Silicon substrates coated with partially amorphous and/or crystalline $CaCO_3$ were soaked in a disodium phosphate Na_2HPO_4 (pure p.a., Chempur) solution (1 mol/l) for 28 days in a thermostat at 80°C.

For the characterisation of surface properties, the X-ray powder diffraction (XRD) analysis, scanning electron microscopy (SEM) and Raman

Table. **Silicon substrate coating techniques**

Parameter	Spinning procedure (A), sec	Spinning procedure (B), sec
RPM1	1000	500
RAMP1	1	2
TIME1	1	5
RPM2	3000	1000
RAMP2	2	2
TIME2	1	5
RPM3	3000	1500
RAMP3	1	2
TIME3	30	90
RAMP4	10	10

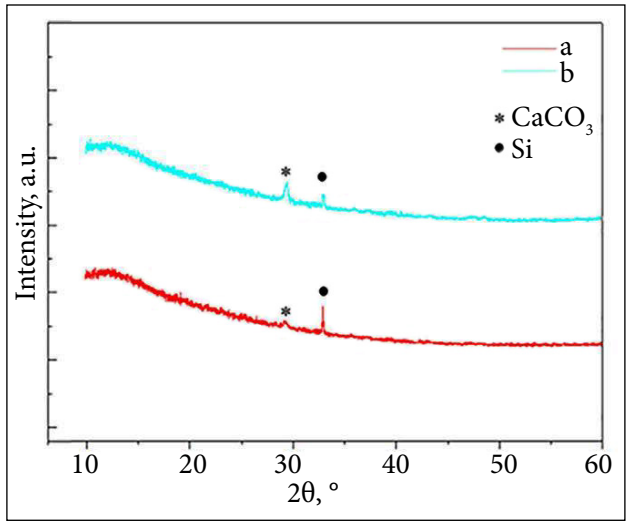

Fig. 1. XRD patterns of the sol-gel derived $CaCO_3$ samples on the Si substrate obtained after 20 coatings and annealed at 600°C for 5 h after each spining procedure, using different (A) and (B) spin-coating techniques

spectroscopy were applied. The XRD studies were performed on a Rigaku miniFlex II diffractometer operating with Cu *K*α1 radiation (start angle 10; stop angle 60; sampling W. 0.010; scan speed 5.0; kV 30). In order to study the morphology and microstructure of the samples a scanning electron microscope Hitachi SU-70 was used. The thickness of HA coatings was measured using the SEM analysis of the cross-sections of films. Raman spectroscopy studies were performed using a scanning near-field spectroscopy system with a Raman spectroscopy accessory (Alpha300R, WiTec). Elemental analysis was performed on a Thermo Fischer Scientific Flash 2000 Elemental Analyzer.

RESULTS AND DISCUSSION

As was mentioned, the silicon substrates were repeatedly coated with the 10, 20 and 30 layers of the sol-gel solution. However, the XRD patterns of the samples obtained after 10 coatings procedures did not contain any reflections attributable to a crystalline $CaCO_3$ phase. Figure 1 represents the XRD patterns of $CaCO_3$ thin films obtained after 20 coatings using slightly different spin-coating procedures. As seen from Fig. 1, the peaks attributable to $CaCO_3$ ($2\theta \approx 29.5$; PDF [96-210-0190]) could be determined in the XRD patterns confirming the formation of crystalline calcium carbonate. Additionaly, the diffraction peak from the substrate Si ($2\theta \approx 33$; PDF [96-901-1057]) is also seen. It is interesting to note that the XRD patterns of $CaCO_3$ layers fabricated after 30 spin-coating procedures were almost identical to the ones presented in Fig. 1.

The SEM micrographs of the surfaces of obtained $CaCO_3$ samples are shown in Fig. 2. The surface of the specimen obtained after 30 spinning times is partially even with the clearly pronounced formation of individual crystallites. The quality of the sol-gel coated thin films of $CaCO_3$ is not influenced by used spin-coating techniques.

The synthesised $CaCO_3$ coatings were also investigated using Raman spectroscopy. The Raman spectra of the synthesised samples are depicted in Fig. 3. The analysis of Raman spectroscopy results shows the characteristic $CaCO_3$ peaks located at 153, 281, 617, 668, 709 and 1084 cm^{-1} formed after 30 coatings using the both spin-coating techniques (A) and (B) [36, 37]. It is interesting to note that the positions of Raman bands determined in the Raman spectra of synthesised $CaCO_3$ according to [36] could be attributed to the partially amorphous calcium carbonate phase.

Calcium hydroxyapatite coatings were synthesised by a low-temperature dissolution-precipitation method. The silicon substrates coated with partially amorphous and/or crystalline $CaCO_3$ were soaked in the disodium phosphate Na_2HPO_4 solution for 28 days at 80°C. Figure 4 presents the XRD patterns of the Si substrate coated initially with $CaCO_3$ following the formation of the calcium phosphate phase. The results of XRD analysis show the negligible influence of the parameters of spinning on the crystallisation of calcium hydroxyapatite on the Si substrate.

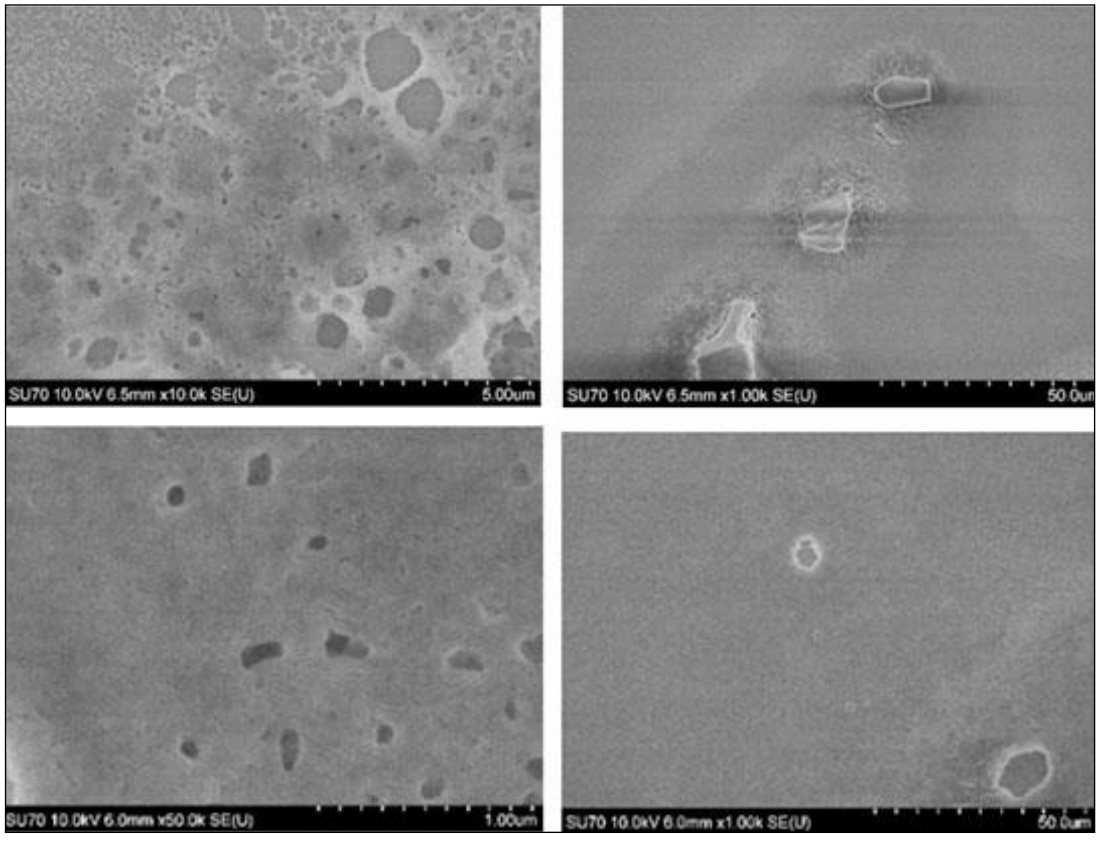

Fig. 2. SEM micrographs of the $CaCO_3$ thin films on the silicon substrate fabricated after 30 coatings using different (A, top) and (B, bottom) spin-coating techniques and obtained at different magnifications

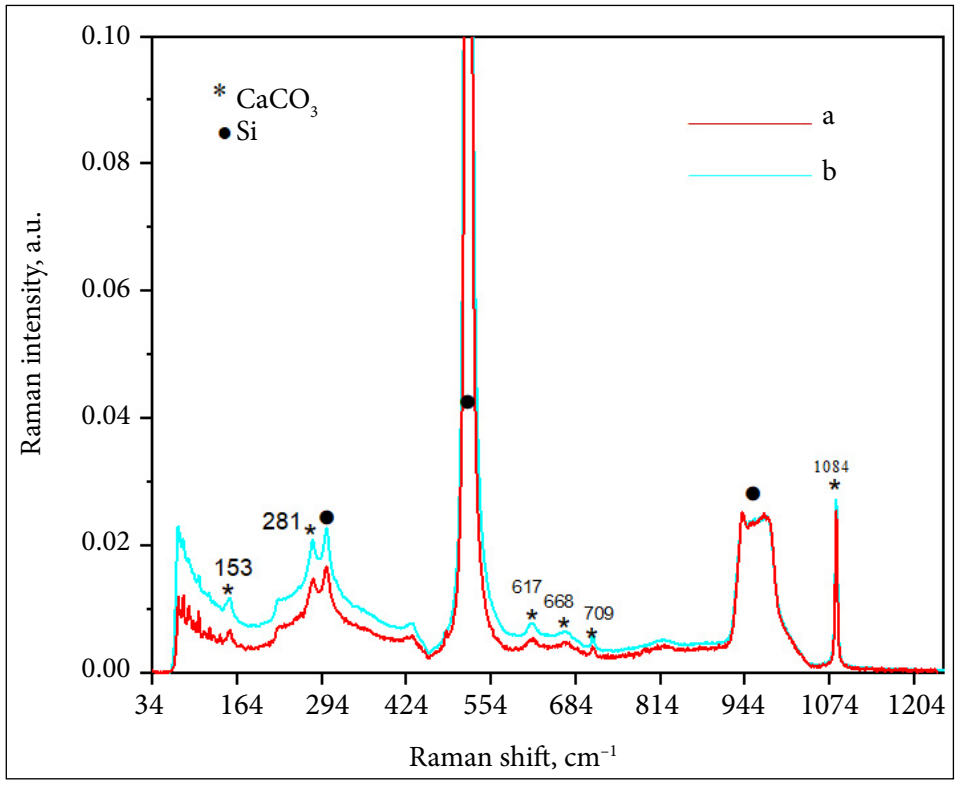

Fig. 3. Raman spectra of the $CaCO_3$ samples containing 30 layers synthesised using different spin-coating techniques: (a) A and (b) B

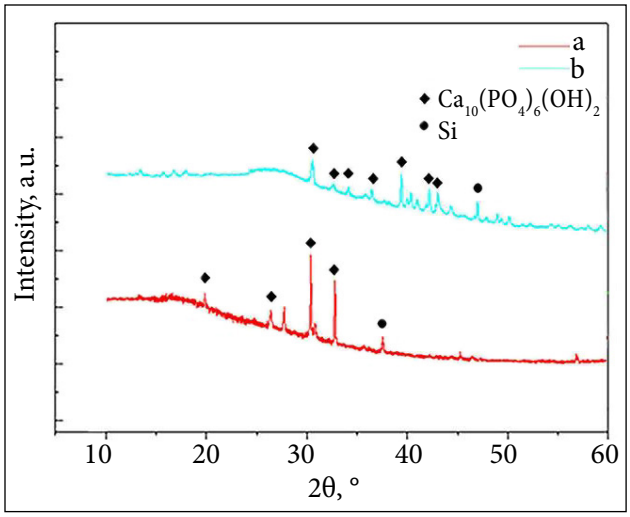

Fig. 4. XRD patterns of the calcium hydroxyapatite thin films fabricated by the sol-gel and dissolution-precipitation method using different spin-coating techniques: (a) A and (b) B

The characteristic HA peaks could be easily distinguished (PDF [74-0566]) despite some reflections originated from the used substrate are also visible. Thus, the data of XRD analysis proved that calcium hydroxyapatite could be easily obtained at 80°C from the Ca-O sol-gel precursor solution on the Si substrate using the spin-coating technique and following dissolution-precipitation approach.

The thickness of HA coatings was measured using the SEM analysis of the cross-sections of films, and was found to be approximately 900–945 nm. The elemental analysis of synthesised products was also performed. No carbon due to a possible formation of carbonate apatite in the synthesis products was detected.

Figure 5 shows the Raman spectra in the wavenumber region from 100 to 1250 cm^{-1} of the CHA sample containing 30 layers of $CaCO_3$ on the Si substrate. The spectra were recorded at the centre of the specimens. The broad bands with sharp peaks near 300, 500 and 950 cm^{-1} belong to the overtone spectrum of Si substrate. However, the intense bands corresponding to the symmetric stretching vibration of phosphate groups in $Ca_{10}(PO_4)_6(OH)_2$ are also seen [38, 39]. The results of Raman spectroscopy are in a good agreement with the XRD analysis data. Using the Raman optical microscopy system in the representative optical images is presented in Fig. 6. The images demonstrate the formation of individual crystallites in the film matrix. By pointing the laser at the formed individual crystallites, HA signals were observed. Defects commonly present in 2D materials, such as cracks, vacancies and crystal boundaries [40, 41], were not detected in the HA

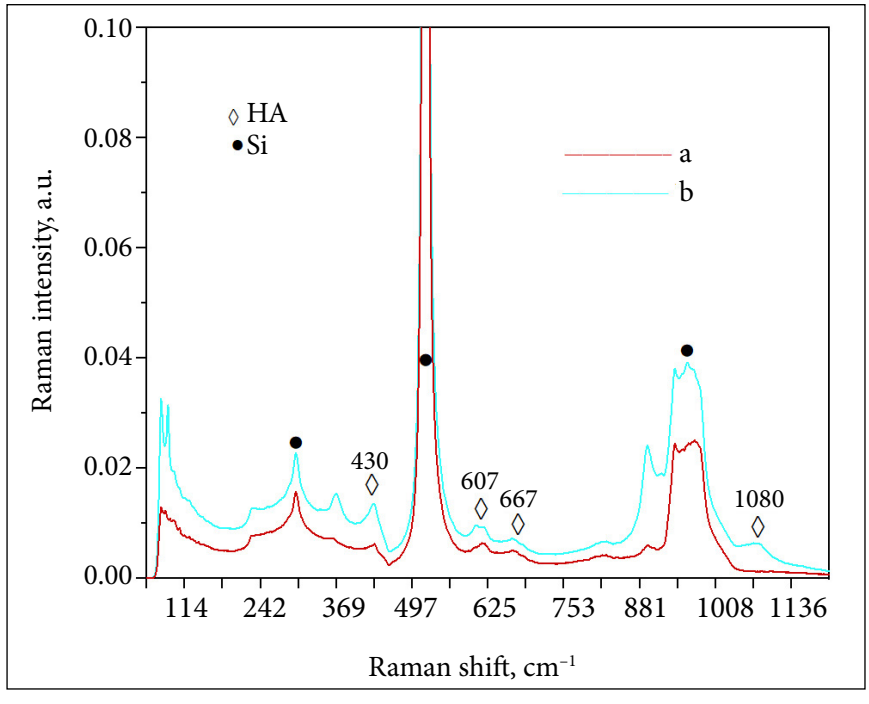

Fig. 5. Raman spectra of the HA synthesised by the sol-gel and dissolution-precipitation method using different spin-coating techniques: (a) A and (b) B

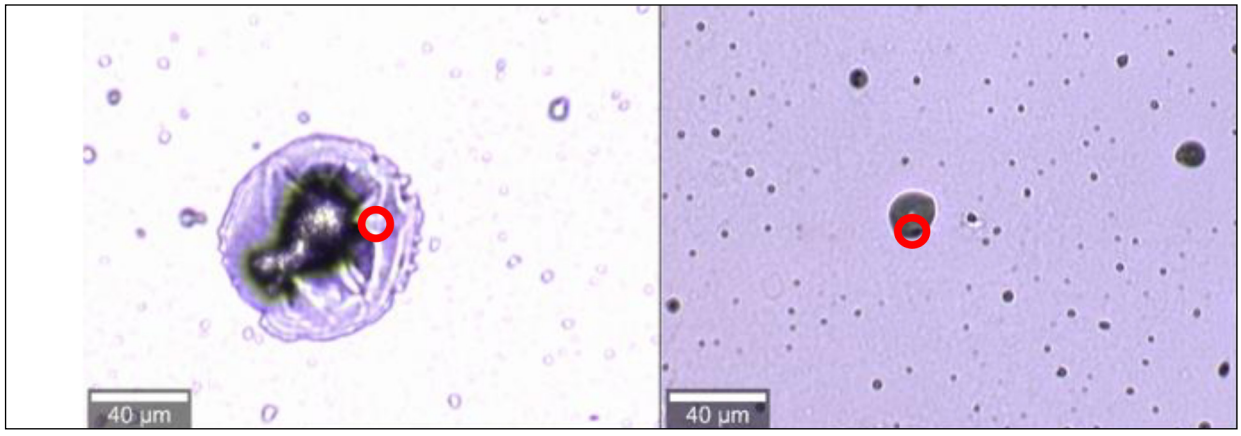

Fig. 6. Images of the HA thin films obtained by Raman optical microscopy system. Red circles mark the location of focused laser beam for measuring Raman spectra

samples synthesised by the low-temperature sol-gel and dissolution-precipitation method.

Thus, the final formation of HA on the surface of Si could be expressed by the following equation [42–44]:

$$10\ CaCO_3 + 6\ PO_4^{3-} + 2\ OH^- \rightarrow$$

$$Ca_{10}(PO_4)_6(OH)_2 + 10\ CO_3^{2-}. \quad (1)$$

The possible mechanism of the formation of calcium hydroxyapatite by the suggested low-temperature sol-gel and dissolution-precipitation method is presented in Fig. 7.

CONCLUSIONS

The wet chemistry route has been developed to prepare calcium hydroxyapatite ($Ca_{10}(PO_4)_6(OH)_2$, HA) thin films on the silicon substrate using for the first time the low-temperature sol-gel and dissolution-precipitation approach. The calcium carbonate thin films on the silicon substrate were obtained by the spin-coating technique when the substrates

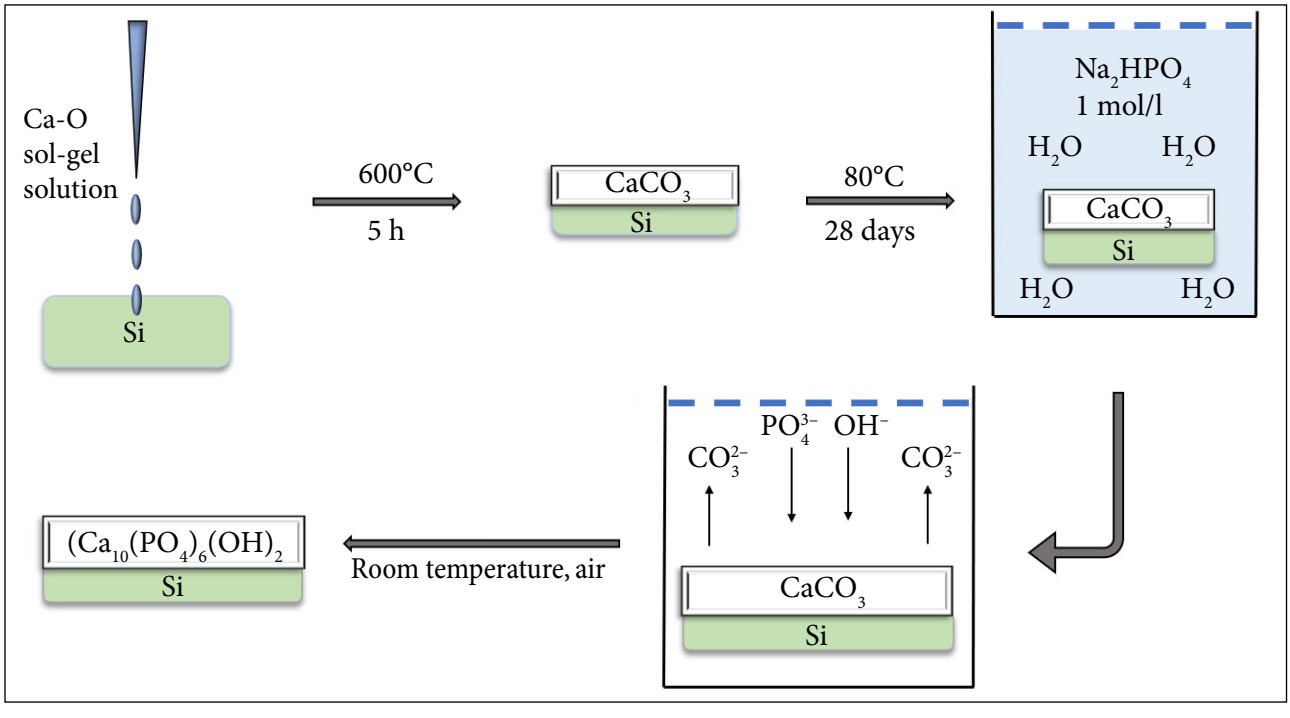

Fig. 7. The possible mechanism of the formation of calcium hydroxyapatite by the suggested low-temperature sol-gel and dissolution-precipitation method on the Si substrate

were repeatedly coated with 10, 20 and 30 layers of the sol-gel solution. It was demonstrated by XRD analysis and Raman spectroscopy that the quality of $CaCO_3$ coatings was not dependent on the spinning rate. The composites formed of crystalline and amorphous $CaCO_3$ were obtained by calcination of the coatings for different times at 600°C. These coatings were used for the fabrication of calcium hydroxyapatite thin films on the silicon substrate using the dissolution-precipitation procedure. The silicon substrates coated with partially amorphous and/or crystalline $CaCO_3$ were soaked in the disodium phosphate Na_2HPO_4 solution for 28 days at 80°C. The data of XRD analysis and Raman spectroscopy again proved that calcium hydroxyapatite could be easily obtained by the developed synthesis method. The possible mechanism of the formation of calcium hydroxyapatite using the low-temperature sol-gel and dissolution-precipitation method was also suggested. It is well known that the main morphological features (particle size, shape and size distribution) of the synthesis products depend very much on the synthesis temperature. The elaborated low-temperature synthesis method for HA coatings would allow a much more efficient control of the surface morphology of the end product.

ACKNOWLEDGEMENTS

This project has received funding from the European Social Fund (Project No. 09.3.3-LMT-K-712-19-0069) under Grant Agreement with the Research Council of Lithuania (LMTLT).

Received 22 February 2022
Accepted 9 March 2022

References

1. T. Habibah, D. Amlani, M. Brizuela, *Hydroxyapatite Dental Material*, StatPearls Publishing, Treasure Island, FL (2018).
2. B. L. Thi, R. Shi, B. D. Long, et al., *Biomed. Mater.*, **15**, 035004 (2020).
3. A. K. Teotia, D. B. Raina, C. Singh, et al., *ACS Appl. Mater. Interf.*, **9**, 6816 (2017).
4. A. Szewczyk, A. Skwira, M. Ginter, D. Tajer, M. Prokopowicz, *Polymers*, **13**, 53 (2021).
5. S. M. Zakaria, S. H. Zein, M. R. Othman, F. Yang, J. A. Jansen, *Tissue Eng. Part B Rev.*, **19**, 431 (2013).
6. T. Debnath, A. Chakraborty, T. K. Pal, *J. Indian Soc. Periodontol.*, **18**, 593 (2014).
7. A. Rogina, M. Antunovic, D. Milovac, *J. Biomed. Mater. Res. B*, **107**, 197 (2019).
8. A. Lode, A. Bernhardt, K. Kroonen, M. Springer, A. Briest, M. Gelinsky, *J. Tissue Eng. Regen. Med.*, **3**, 149 (2009).
9. M. Kumar, R. Kumar, S. Kumar, *Mater. Today Proc.*, **45**, 5269 (2021).
10. Y. Cheng, G. Zhao, H. Liu, *Zhongguo Xiu Fu Chong Jian Wai Ke Za Zhi*, **12**, 74 (1998).
11. J. Park, B. J. Kim, J. Y. Hwang, et al., *J. Nanosci. Nanotechnol.*, **18**, 837 (2018).
12. P. Shi, M. Liu, F. Fan, C. Yu, W. Lu, M. Du, *Mater. Sci. Eng. C*, **90**, 706 (2018).
13. Z. Stankevičiūtė, M. Malakauskaitė, A. Beganskienė, A. Kareiva, *Chemija*, **24**, 288 (2013).
14. V. Wagener, A. R. Boccaccini, S. Virtanen, *Appl. Surf. Sci.*, **416**, 454 (2017).
15. Y. Y. Su, K. Z. Li, L. L. Zhang, C. C. Wang, Y. P. Zhang, *Surf. Coat. Technol.*, **352**, 619 (2018).
16. L. F. Sukhodub, L. B. Sukhodub, W. Simka, M. Kumeda, *Mater. Lett.*, **250**, 163 (2019).
17. V. T. Nguyen, T. C. Cheng, T. H. Fang, M. H. Li, *J. Mater. Res. Technol.*, **9**, 4817 (2020).
18. K. Ishikawa, A. Kareiva, *Chemija*, **31**, 25 (2020).
19. S. F. Wen, X. L. Liu, J. H. Ding, et al., *Progr. Nat. Sci.*, **31**, 324 (2021).
20. D. Avnir, T. Coradin, O. Lev, J. Livage, *J. Mater. Chem.*, **16**, 1013 (2006).
21. P. Usinskas, Z. Stankeviciute, G. Niaura, J. Ceponkus, A. Kareiva, *Mater. Sci.–Medžiagotyra*, **25**, 365 (2019).
22. V. Jonauske, R. Ramanauskas, R. Platakyte, et al., *Mendeleev Commun.*, **30**, 512 (2020).
23. K. Ishikawa, E. Garskaite, A. Kareiva, *J. Sol-Gel Sci. Technol.*, **94,** 551 (2020).
24. R. Gibson, in: *Biomaterials Science*, 4th edn., An Introduction to Materials in Medicine, 307, Academic Press (2020).
25. F. K. Basak, E. Kayahan, *Ceram. Int.*, **47**, 27880 (2021).
26. A. A. Ahmad, A. M. Alsaad, *Bull. Mater. Sci.*, **30**, 301 (2007).
27. J. Y. Cha, C. H. Kim, Y. J. Kim, *J. Ceram. Soc. Jpn.*, **126**, 940 (2018).
28. B. Hiebl, C. Hopperdietzel, H. Huenigen, F. Jung, N. Scharnagl, *Clin. Hemorheol. Microcirc.*, **55**, 491 (2013).
29. J. T. Jeong, M. K. Choi, Y. Sim, et al., *Sci. Rep.*, **6**, 33835 (2016).
30. S. L. Iconaru, A. Groza, S. Gaiaschi, et al., *Coatings*, **10**, 1124 (2020).
31. R. M. do Nascimento, A. J. de Paula, N. C. Oliveira, et al., *Mater. Sci. Eng. C*, **94**, 417 (2019).
32. Z. V. Parlak, S. Wein, R. Zybala, et al., *J. Biomater. Appl.*, **34**, 585 (2019).

33. J. Friguglietti, S. Das, P. Le, et al., *Biomaterials*, **244**, 119927 (2020).
34. S. Petrovic, D. Perusko, A. Mimidis, et al., *Nanomaterials*, **10**, 2531 (2020).
35. A. Zarkov, A. Stanulis, J. Sakaliuniene, et al., *J. Sol-Gel Sci. Technol*., **76**, 309 (2015).
36. M. M. Tlili, M. Ben Amor, C. Gabrielli, et al., *J. Raman Spectrosc*., **33**, 10 (2001).
37. A. Dandeu, B. Humbert, C. Carteret, H. Muhr, E. Plasari, J.-M. Bossoutrot, *Chem. Eng. Technol*., **29**, 221 (2006).
38. G. B. Ramirez-Rodriguez, J. M. Delgado-Lopez, J. Gomez-Morales, *CrystEngComm*, **15**, 2206 (2013).
39. S. Koutsopoulos, *J. Biomed. Mater. Res*., **62**, 600 (2002).
40. F. Zhong, H. Wang, Z. Wang, et al., *Nano Res*., **14**, 1840 (2021).
41. J. F. Schultz, S. W. Li, S. Jiang, N. Jiang, *J. Phys. Condens. Matter*, **32**, 463001 (2020).
42. K. Ishikawa, *Materials*, **3**, 1138 (2010).
43. I. Grigoraviciute-Puroniene, Y. Tanaka, V. Vegelyte, Y. Nishimoto, K. Ishikawa, A. Kareiva, *Ceram. Int*., **45**, 15620 (2019).
44. R. Kishida, M. Elsheikh, K. Hayashi, A. Tsuchiya, K. Ishikawa, *Ceram. Int*., **47**, 19856 (2021).

Rasa Karalkevičienė, Greta Briedytė, Tomas Murauskas, Mantas Norkus, Aleksej Žarkov, Jen-Chang Yang, Aivaras Kareiva

NAUJAS BIOKERAMINIŲ NANOKALCIO HIDROKSIAPATITO DANGŲ FORMAVIMO METODAS NAUDOJANT ZOLIŲ-GELIŲ IR TIRPINIMO-NUSODINIMO PROCESUS

S a n t r a u k a

Šiame darbe kalcio hidroksiapatito ($Ca_{10}(PO_4)_6(OH)_2$, (HA)) plonos plėvelės ant silicio padėklo susintetintos taikant naują žematemperatūrį zolių-gelių ir tirpinimo-nusodinimo metodą. Iš pradžių ant silicio padėklo buvo gautos $CaCO_3$ dangos kaitinant zolius-gelius skirtingą laiką 600 °C temperatūroje. Kalcio hidroksiapatito plonoms plėvelėms paruošti ant silicio padėklo 80 °C temperatūroje buvo naudota tirpinimo-nusodinimo procedūra. Gauti sintezės produktai apibūdinti remiantis rentgeno spindulių difrakcijos analize, skenuojančia elektronų mikroskopija ir Ramano spektroskopija. Taip pat buvo pasiūlytas galimas kalcio hidroksiapatito susidarymo mechanizmas.